

Article

Performance Evaluation of PVD and CVD Multilayer-Coated Tools in Machining High-Strength Steel

Saima Yaqoob ^{1,2}, Jaharah A. Ghani ¹, Nabil Jouini ^{3,4,*} and Afifah Z. Juri ¹

¹ Department of Mechanical and Manufacturing Engineering, Faculty of Engineering and Built Environment, Universiti Kebangsaan Malaysia, Bangi 43600, Selangor, Malaysia; engg_saima@hotmail.com (S.Y.); jaharahghani@ukm.edu.my (J.A.G.); afifahjuri@ukm.edu.my (A.Z.J.)

² Department of Industrial and Manufacturing Engineering, NED University of Engineering and Technology, University Road, Karachi 75270, Pakistan

³ Mechanical Engineering Department, College of Engineering, Prince Sattam Bin Abdulaziz University, Alkharj 11942, Saudi Arabia

⁴ Laboratoire de Mécanique, Matériaux et Procédés (LR99ES05), École Nationale Supérieure d'Ingénieurs de Tunis, Université de Tunis, Tunis 1008, Tunisia

* Correspondence: n.jouini@psau.edu.sa

Abstract: To curtail the negative effects of traditional flood machining, dry cutting using carbide tools has emerged as a prominent alternative for manufacturers, owing to its low cost and phenomenal surface qualities. In line with this view, high-speed machining of high-strength AISI 4340 alloy steel was carried out using multilayer Al₂O₃/TiCN-CVD and TiAlN/AlCrN-PVD carbide tools in a dry environment. The experimental scheme was adopted, as per Taguchi's L₁₈ orthogonal array, to investigate the two most crucial machinability aspects, namely tool life and surface roughness. An analysis of variance (ANOVA) was performed on the obtained data, and it was inferred that the feed rate exhibited the strongest effects on both the tool life and surface roughness, with corresponding percentage contributions of 46.22% and 68.96%, respectively. The longest tool lives of 14.75 min and 10.08 min were obtained at a low cutting speed and feed rate for CVD and PVD tools, respectively. However, the lowest surface roughness of 0.276 μm and 0.307 μm was achieved at a high cutting speed and low feed rate for PVD and CVD tools, respectively. The evolution of tool wear, studied through the microscopic images of the worn tools, revealed that a high cutting speed and feed rate accelerated the flank wear for both types of tools. Nevertheless, the CVD tool exhibited better results due to the thick and effective Al₂O₃/TiCN coating layer, which protected the carbide substrate against thermal-mechanical loads. Moreover, scanning electron microscopy (SEM) and energy-dispersive X-ray spectroscopy (EDX) performed on the worn tools revealed that adhesion, oxidation, diffusion, and abrasion were the main wear mechanisms for both types of tools.



Citation: Yaqoob, S.; Ghani, J.A.; Jouini, N.; Juri, A.Z. Performance Evaluation of PVD and CVD Multilayer-Coated Tools in Machining High-Strength Steel. *Coatings* **2024**, *14*, 865. <https://doi.org/10.3390/coatings14070865>

Academic Editors: Emmanuel P. Georgiou and Angelos Koutsomichalis

Received: 12 June 2024

Revised: 2 July 2024

Accepted: 4 July 2024

Published: 10 July 2024



Copyright: © 2024 by the authors. Licensee MDPI, Basel, Switzerland. This article is an open access article distributed under the terms and conditions of the Creative Commons Attribution (CC BY) license (<https://creativecommons.org/licenses/by/4.0/>).

Keywords: high-speed machining; multilayer-coated carbide tool; AISI 4340; surface roughness; tool wear; tool life

1. Introduction

In this era of rapid development, manufacturing industries remain the main source of environmental pollution. The precarious effluents produced by the industrial sector, when released into the atmosphere, pose serious environmental and health hazards. Metal cutting is a critical manufacturing process that relies heavily on lubricants. However, conventional metal-cutting fluids, while effective at suppressing heat, pose severe medical and ecological risks. Studies have linked exposure to conventional metal-cutting fluids to an increased risk of various types of cancer, skin allergies, and even physical disabilities [1]. Moreover, their chemical dissolution after disposal is a potential cause of soil contamination and water pollution, emphasizing the need for expensive, yet necessary, pre-disposal treatment [2]. According to statistics presented by a leading German automobile company, the

procurement and disposal expenses associated with cutting fluids make up approximately 7% to 17% of the direct labor cost [3]. Due to these ecological and economic challenges, dry cutting has emerged as a growing field of research. Dry cutting, being carried out without coolants or lubricants, offers significant environmental advantages over flood machining. However, the involvement of high thermal–mechanical loads, particularly in the machining of difficult-to-cut materials, such as titanium, nickel, and high-strength steel, compromises surface quality and the dimensional accuracy of machined components in a dry environment [4]. To address these challenges, advanced tool materials and coatings possessing excellent tribological properties and wear resistance have been introduced. Although the application of advanced materials such as ceramics, cubic boron nitride (CBN), and polycrystalline cubic boron nitride (PCBN) have substantially improved the chemical, mechanical, and cutting capabilities of cutting tools, cemented carbide tools, due to their cost-effectiveness, still capture a major share (~53%) of the market [5]. Among these, 80%–90% are categorized with single- or multilayer-coated carbide tools [6]. Thin films covering the surface of a carbide substrate function as hard coatings and serve various purposes. For instance, coating a substrate with a highly thermally resistant material can protect it from temperature-driven damage in applications involving elevated temperatures [7]. Grigoriev et al. [2] reported that Ti-based coatings can withstand high machining temperatures and considerably inhibit the diffusion and oxidation wear mechanism.

The most common types of hard coatings that are applied to cutting tools are TiCN, HSN², Al₂O₃, TiN, TiAlN, TiB₂, TiBN, and AlTiCrN [8]. The synthesis of coatings can generally be achieved through physical vapor deposition (PVD) and chemical vapor deposition (CVD) processes. Both techniques differ in their method of application and depend on the type and nature of the coating and substrate material. PVD refers to a vacuum-coating process that allows for the deposition of solid material as a thin film layer on the substrate body through vaporization and condensation [9]. The coating temperature in PVD remains lower than 500 °C, and a thin layer of coated material is deposited on the base material, making it mostly suitable for finishing applications [7]. On the other hand, CVD is a heat-activated process in which gaseous precursors are injected into a reaction chamber for chemical surface reaction and dissociation, resulting in the formation of a potential coating. The temperature of the substrate is maintained between 800 °C and 1150 °C [10]. Both deposition methods can form single-layer and multilayer coatings. The effectiveness of single- and multilayer coating has also been investigated by many researchers; multilayer coatings have been claimed to be more effective when machining difficult-to-cut materials. Chinchankar and Choudhury [11] reported that coated tools can substantially reduce tool wear mechanisms. They noticed a significant reduction in tool wear when a single-layer TiAlN-coated tool was compared with an uncoated tool while machining hardened steel, demonstrating satisfactory performance in increasing cutting from 62 to 200 m/min. However, the cutting efficiency of multilayer TiCN/Al₂O₃/TiN tools was remarkably improved up to a cutting speed of 350 m/min. It was concluded that single-layer coatings could not sustain the harsh machining environment and were, thus, severely affected by accelerated crater wear, weakening the cutting edge.

High-strength steel has widespread engineering applications (e.g., transmission shafts, gears, bearings, rolling dies, building structures, pipeline transportation, etc.) due to its superior qualities, such as high hardness and torsional strength, enhanced fatigue and abrasion resistance, and excellent shock-absorbing abilities [12,13]. Moreover, its high abrasiveness, low thermal conductivity, and high plastic nature are associated with poor machining capabilities [14]. The high cutting resistance exhibited by heat-treated steel, particularly at high machining regimes, is the leading cause of intense heat generation, high power consumption, unfavorable chip formation, shorter tool life, and increased machining time and cost [15]. With advancements in coating technologies, these machinability challenges can be addressed. The literature has reported that abrasion, adhesion, and temperature-driven diffusion are the main tool wear mechanisms in the machining of AISI 4340 high-strength alloy steel [16,17]. Therefore, Al₂O₃ coatings, being thermally

and chemically resistant [18], can be paired with TiCN [19] or TiAlN coatings, which are categorized by high adhesion and corrosion resistance [20], to provide a better machinability performance. According to Li et al. [21], multilayer PVD-coated carbide tools can improve the machinability of heat-treated alloy steel during a high-speed machining process. They employed three types of PVD coatings, namely AlTiN single-layer, TiAlN/TiN bi-layer, and TiN/TiCN/TiAlN multilayer coatings, on the carbide substrate and a PVD bi-layer-TiCN/NbC composite coating on the ceramic substrate. It was reported that TiN/TiCN/TiAlN tools considerably reduced the tearing and collapse of the coatings and resulted in less plastic deformation, crack nucleation, edge chipping, and abrasive wear.

Many studies have been carried out regarding the machining of high-strength steel, with different coatings and tool materials. Das et al. [22] utilized thin multilayer Ti (C N O) PVD-coated cermet tools in machining heat-treated AISI 4340 alloy steel and achieved the lowest surface roughness of $1.065 \mu\text{m}$ in cutting speed, $V = 250 \text{ m/min}$, feed rate, $F = 0.09 \text{ mm/rev}$, and depth of cut, $\text{DOC} = 0.4 \text{ mm}$. Interestingly, they found that the cutting depth was the most influential factor affecting the surface roughness, followed by the feed rate and cutting speed. However, Zheng et al. [23], in the milling of AISI 4340 (43 HRC) steel using an $\text{Al}_2\text{O}_3/\text{TiCN}$ CVD-coated carbide tool, found considerably less surface roughness, $0.40 \mu\text{m}$, at an identical machining speed and feed rate ($V = 250 \text{ m/min}$, $F = 0.09 \text{ mm/rev}$) but with a low depth of cut, $\text{DOC} = 0.1 \text{ mm}$. The performance of a TiAlN PVD-coated tool in machining Ni-based super-alloy was evaluated in reference [24]. The results showed that the TiAlN coating initially suppressed the adherence of the work material, but, with subsequent cutting, crack initiation led to the occurrence of flaking and exposure of the substrate. The literature has also highlighted the comparative studies of different types of coatings. For instance, Sonawane and Sargade [25] compared uncoated AlTiCrN and AlTiN tungsten carbide inserts in turning duplex stainless-steel 2205 under a dry environment. It was reported that AlTiCrN exhibited the lowest amount of tool wear, $V_b = 0.16 \text{ mm}$, after completing 2450 mm of machining length for each tool. Likewise, Boing et al. [6] conducted a comparative assessment of TiCN/ $\text{Al}_2\text{O}_3/\text{TiN}$ CVD and TiAlN PVD multilayer-coated tools, during which they reported the sequence of events of tool wear progression. It was observed that CVD tools were initially affected by abrasion, followed by crack nucleation and propagation, coating delamination, and, lastly, complete spalling. In contrast, the sequence of tool wear events for PVD tools included abrasion, high plastic deformation, crack nucleation, leading to weakening of the substrate and coating bonding, and, eventually, the detachment of the entire coating. In a recent study, Bag et al. [26] reported the best surface quality of machined surfaces ($R_a = 0.40 \mu\text{m}$) with a TiN/TiCN/ Al_2O_3 CVD-coated tool at a cutting speed of 260 m/min . An ANOVA performed on surface roughness data revealed that the feed rate had the highest percentage contribution rate (PCR) of 71.93%, making it the most influential parameter. This was followed by machining speed, with a PCR of 14.8%, and depth of cut, with a PCR of 3.4%. Moreover, they analyzed worn tools and reported abrasion and adhesion as the main wear mechanisms. An ANOVA on tool wear data demonstrated the dominating effect of cutting speed, exhibiting the highest PCR of 66.06%, followed by the feed rate at 13.91% and depth of cut at 3.83%. Alok et al. [27] also acknowledged the highest statistical influence of the cutting speed on flank wear while machining AISI 4340 steel (52 HRC) using a HSN²-coated carbide insert. Furthermore, Kumar et al. [28] investigated the influence of different lubrication conditions, namely water-soluble, nano-cutting fluid, and compressed air, on the cutting performance of uncoated cermet tools. It was determined that nano-cutting fluid effectively reduced the cutting force, produced curlier chips, and inhibited the tool flank wear compared to the other two conditions. These results were in line with the findings of Singh et al. [29], who utilized uncoated textured carbide inserts under nano-fluid-based MQL lubrication. In another study, Zenjanab et al. [30] conducted high-speed machining in a range between $V = 300$ and 400 m/min , $F = 0.1\text{--}0.2 \text{ mm/rev}$, using ceramic tools under dry conditions, CuO-based cutting fluids, and soluble cutting fluids. The results revealed

that CuO-based cutting fluids exhibited better machinability under all cutting conditions due to favorable anti-friction and anti-wear properties.

Shalaby and Veldhuis [31] suggested that pure alumina + ZrO₂-based ceramic tools produced better tool life at a low machining speed, $V = 150$ and 250 m/min, while mixed alumina + Al₂O₃ + TiCN-based ceramic outperformed, with a high cutting speed at $V = 700$ and 1000 m/min. Furthermore, Suyama and Diniz [32] performed high-speed turning of AISI 4340 using a CBN + Al₂O₃/TiCN ceramic phase insert and obtained the longest tool life of 15 min at a low cutting speed of 300 m/min. Additionally, they studied the effect of vibration on tool wear by varying the tool overhang distance and reported that diffusion was the main wear mechanism at high vibration, while abrasion predominated at low vibration. Da Silva et al. [33] compared the results of hard turning with the traditional grinding process by using ceramic and polycrystalline cubic boron nitride (PCBN) tools. It was claimed that hard turning in dry cutting conditions with both tools produced the lowest Ra of $0.18 \mu\text{m}$ at a high cutting speed, $V = 300$ m/min. On the contrary, there was a comparatively high Ra in grinding ($0.20 \mu\text{m}$), suggesting that hard turning could be a potential replacement for the traditional grinding process.

After reviewing the literature, it was determined that tools made up of advanced materials such as CBN and ceramics were primarily evaluated for the high-speed hard machining of AISI 4340 alloy steel. However, the utilization of multilayer-coated carbide tools has not been investigated in detail under high machining parameters. Therefore, this study aimed to provide an in-depth analysis on the performance of multilayer CVD and PVD-coated carbide tools in a dry environment, considering two crucial machinability aspects: surface roughness and tool life. Moreover, the evolution of tool wear and the behavior of different coatings in inhibiting the wear progression, followed by a comprehensive analysis of wear mechanisms, were also included in the scope of this study. It was anticipated that this research would be of potential interest to tool manufacturers and industry professionals who are striving to achieve better product quality and machinability performance by utilizing sustainable methods of manufacturing.

2. Materials and Methods

Round cylindrical bars of AISI 4340 alloy steel having dimensions $\text{Ø}60 \times 120$ were employed for experimentation. The work samples were heat-treated to achieve the desired hardness of 50 HRC through a series of repetitive operations, including 3 h of curing at 840 °C , followed by 1 h of quenching at 830 °C and 4 h of annealing at 400 °C . The experiments were conducted on a CNC turning machine with high cutting speed in a range between 300 and 350 m/min, feed rate 0.05–0.15 mm/rev, and depth of cut 0.1–0.3 mm according to Taguchi L₁₈ orthogonal array, as presented in Table 1. The machining parameters were selected as per Ref. [30], utilizing ceramic tools in high-speed (250–400 m/min) machining of heat-treated AISI 4340 alloy steel (52 HRC), using soluble cutting fluid-based nanofluids (CuO, CuO + boric acid), which have a detrimental impact on the environment. This study was conducted to realize sustainable machining using a dry approach and aimed to evaluate the effectiveness of multilayer-coated carbide tools, which are less costly than ceramic tools.

Two multilayer-coated carbide inserts TiAlN/AlCrN with physical vapor deposition (PVD) and Al₂O₃/TiCN chemical vapor deposition (CVD) were employed for the turning experiments. The selection of tool coating was based on reviewed literature, as hard turning generates intense machining heat, which promotes temperature-driven wear mechanisms. Therefore, effective coatings were selected to provide thermal stability and chemical resistance. For instance, Al₂O₃ coating forms a thermal barrier and offers greater oxidation and wear resistance at elevated temperatures [34], TiCN exhibits resistance to shock loading [21], TiAlN coating possesses hardness and self-lubricating properties [35], and TiCrN offers good wear resistance and chemical stability [36]. The characteristics of both tools are listed in Table 2. Tool performance was evaluated by measuring tool wear and surface roughness under each experimental condition. The progression of tool wear was tracked by capturing

the wear images at different intervals using a Zeiss Stemi 2000-C optical microscope (Zeiss, Oberkochen, Germany), where an average tool life criterion of $V_b \geq 300 \mu\text{m}$ was used as per ISO 3685 [37] for tool life analysis. Next, the worn inserts were analyzed using a Zeiss SUPRA 55VP scanning electron microscope (SEM) and energy-dispersive spectroscopy (EDS) to determine the associated wear mechanisms. Then, the surface quality of machined samples was measured by using a Mitutotyo Surfesst SJ-301 surface roughness tester (Mitutotyo, Kawasaki, Japan). Three surface roughness readings were recorded at different positions on the cylindrical workpiece, and the average value was computed. Figure 1 illustrates the experimental scheme adopted for this study.

Table 1. Experimental scheme, as per Taguchi L_{18} .

Exp. No	Tool Type (T)	Cutting Speed V (m/min)	Feed Rate F (mm/rev)	Depth of Cut DOC (mm)	Exp. No	Tool Type (T)	Cutting Speed V (m/min)	Feed Rate F (mm/rev)	Depth of Cut DOC (mm)
E1	PVD	300	0.05	0.1	E10	CVD	300	0.05	0.3
E2	PVD	300	0.10	0.2	E11	CVD	300	0.10	0.1
E3	PVD	300	0.15	0.3	E12	CVD	300	0.15	0.2
E4	PVD	350	0.05	0.1	E13	CVD	350	0.05	0.2
E5	PVD	350	0.10	0.2	E14	CVD	350	0.10	0.3
E6	PVD	350	0.15	0.3	E15	CVD	350	0.15	0.1
E7	PVD	400	0.05	0.2	E16	CVD	400	0.05	0.3
E8	PVD	400	0.10	0.3	E17	CVD	400 </td <td>0.10</td> <td>0.1</td>	0.10	0.1
E9	PVD	400	0.15	0.1	E18	CVD	400	0.15	0.2

Table 2. Characteristics of PVD and CVD tools [38].

Characteristics	PVD Tool	CVD Tool
Grade	H-grade	P-grade
Coating	TiAlN/AlCrN	Al ₂ O ₃ /TiCN
Coating thickness	3 μm	18 μm
Hardness of substrate	93.2 HRA	90.5 HRA
Nose radius	0.4 mm	0.4 mm
Rake angle	-6°	-6°
Cutting edge angle	95°	95°

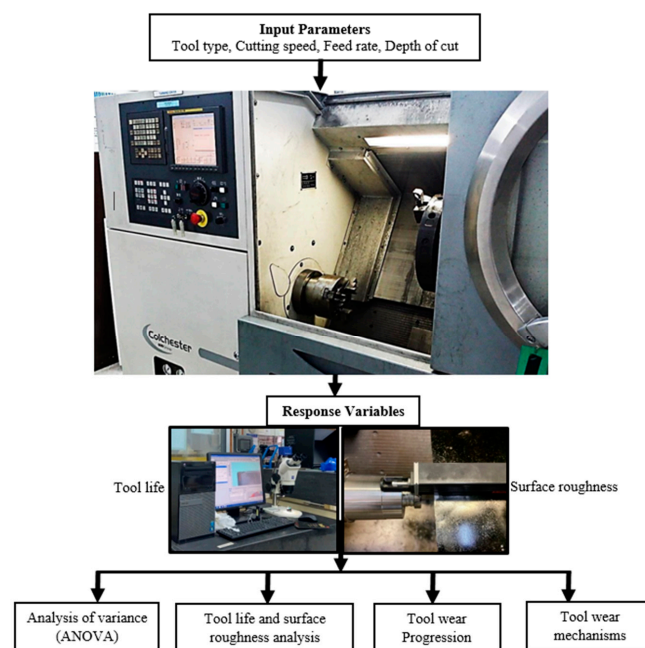


Figure 1. Experimental setup adopted for machining.

3. Results and Discussion

This section presents a comprehensive discussion on the crucial machinability aspects when high-strength steel was machined with Al₂O₃/TiCN-CVD and TiAlN/AlCrN-PVD carbide tools: tool life, tool wear progression, tool wear mechanisms, and surface roughness.

3.1. Statistical Analysis of Tool Life and Surface Roughness

The output variables tool life and surface roughness for each experimental run are tabulated in Table 3. Analysis of variance (ANOVA) was performed to infer meaningful information from the obtained data, and the most significant factors with their percentage contributions were determined by using Minitab 17 statistical software.

Table 3. Results obtained for each experimental run.

Exp. No	Tool Type	Surface Roughness	Tool Life	Exp. No	Tool Type	Surface Roughness	Tool Life
E1	PVD	0.3490	10.080	E10	CVD	0.4910	14.750
E2		1.0800	6.590	E11		0.8320	10.570
E3		1.9723	2.980	E12		1.2110	4.540
E4		0.2755	7.830	E13		0.3050	14.110
E5		1.1660	3.290	E14		0.7190	6.850
E6		1.7430	1.940	E15		0.9920	2.840
E7		0.2940	4.530	E16		0.3070	4.830
E8		0.7210	0.943	E17		0.5820	4.230
E9		1.2060	0.493	E18		0.7940	2.510

3.1.1. Tool Life

Based on the ANOVA results (Table 4), it was revealed that the feed rate, cutting speed, and tool type were the most influential parameters for tool life, with corresponding percentage contributions of 46.22%, 28.50%, and 12.92%, respectively. However, the depth of cut with $p = 0.828$ was found to be insignificant, and its contribution was only 0.46%. Similar results could also be deduced from the main effect plot of the means in Figure 2a, where the depth of cut showed a relatively shorter spread in comparison to other parameters. The result of the present study was unexpected based on the previous literature, where, generally, the cutting speed was the governing factor for tool life. The appreciable variation in tool life with changing feed rates can be justified by the fact that raising the feed rate leads to an increased tool–workpiece contact area, resulting in a high material removal rate. This exerts more force on the tool, in addition to a colossal increase in friction between the contacting surfaces. These factors substantially contributed in hastening the tool wear, particularly in the hard turning operation, which unequivocally involves high thermal stresses. Therefore, the range of variation in tool life was sufficient to contribute greater weight to the feed rate, and this nullified the presumed dominating influence of machining speed. The results obtained in this research were similar to López-Luiz et al. [39], who performed hard turning of AISI D2 steel with carbide inserts and found the feed rate to be the most controlling factor affecting the tool wear/life. Moreover, a recent study carried out by Fedai [40] in turning AISI 4340 alloy steel also found the feed rate to be a statistically significant exerting dominating effect on tool wear rather than cutting speed. Overall, the upward trend demonstrated by the CVD-coated tools in the main effect plot of tool type in Figure 2a showed that they outperformed in extending tool life within the conducted experimental scheme.

Table 4. ANOVA table for response variables.

Source	DF	Seq SS	Adj SS	Adj MS	F	<i>p</i>	% Cont.	Significance
Tool life (T) (R-Sq 86.62%)								
T	1	39.144	39.144	39.144	10.85	0.008 *	12.92%	Significant
V	2	86.382	86.382	43.191	11.97	0.002 *	28.50%	Significant
F	2	140.08	140.080	70.040	19.41	0.000 *	46.22%	Significant
DOC	2	1.386	1.386	0.6928	0.19	0.828	0.46%	Insignificant
Residual Error	10	36.075	36.075	3.6075				
Total	17	303.067						
Surface Roughness (Ra) (R-Sq 88.09%)								
T	1	0.3680	0.3680	0.36802	11.13	0.008 *	8.75%	Significant
V	2	0.3526	0.3526	0.17631	5.33	0.027 *	8.38%	Significant
F	2	2.8996	2.8996	1.44978	43.83	0.000 *	68.98%	Significant
DOC	2	0.2523	0.2523	0.12614	3.81	0.059	6.002%	Insignificant
Residual Error	10	0.3308	0.3308	0.03308				
Total	17	4.2033						

* Significant factor.

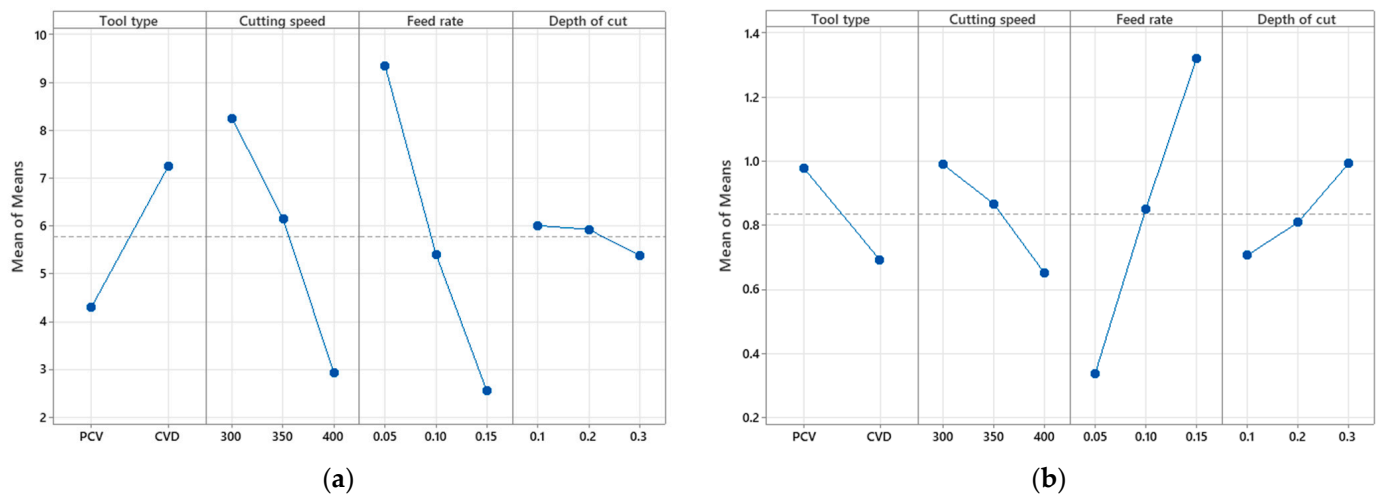


Figure 2. Main effect plot of (a) mean of tool life and (b) mean of surface roughness.

3.1.2. Surface Roughness

The results presented in Table 4 indicate that the feed rate continued to be the most significant factor affecting the surface roughness, exhibiting a percentage contribution of 68.98%. This was followed by cutting speed and tool types, with respective contributions of 8.75 % and 8.38%. However, depth of cut, with *p*-value = 0.059 and contributing 6%, remained the least significant factor in this study. The main effect plot of the mean in Figure 2b also supports these findings, showing that the graph of feed rate, cutting speed, and tool type exhibited a relatively broader spread compared to the depth of cut. The apparent reason for the increasing surface roughness with increasing feed rate is associated with the high chip volume and thrust force, which can lead to increased vibration and, consequently, decreased surface quality. This result is similar to the observation of Mia et al. [41] while machining heat-treated AISI 1060 steel. According to them, the feed rate and then the cutting speed were the most significant governing variables for surface roughness. The lowest mean value exhibited by CVD tools in Figure 2b indicated their superior performance within the conducted experimental scheme.

3.2. Analysis of Tool Life/Wear for PVD- and CVD-Coated Carbide Tool

3.2.1. Tool Life and Tool Wear Progression

From the results illustrated in Figure 3, it was determined that the CVD-coated tool demonstrated the longest tool life of 14.75 min in experiment 10. However, at an identical machining speed ($V = 300$ m/min) and feed rate ($F = 0.05$ mm/rev), the useful life of the PVD-coated tool was 10.08 min, which was 31.3% less than the CVD tool. The trend of decreasing tool life was noticed when increasing the speed and feed for both types of tools. The higher order of both parameters produced significant heat generation and plastic deformation [42]. Overall, CVD-coated tools outperformed PVD tools in all experimental runs, as deduced from Figure 2. The obtained results of tool life can be comprehensively explained by analyzing the tool wear progression and mechanism with different parametric settings. Thorough analysis of tool wear progression can provide valuable insights into potential tool failures. The effects of significant input variables for a comparative assessment of tool wear were evaluated from the Taguchi L_{18} orthogonal array. As in Taguchi's L_{18} design of experiment, only one factor varied, while others remained the same. Since, the depth of cut had been identified as the least influential variable, as per the discussion in Section 3.1.1, its variation was not expected to significantly influence the accuracy of the comparative assessment. Hence, the assessments of tool wear for both CVD and PVD tools were performed by examining the microscopic images of the tool with increasing machining time.

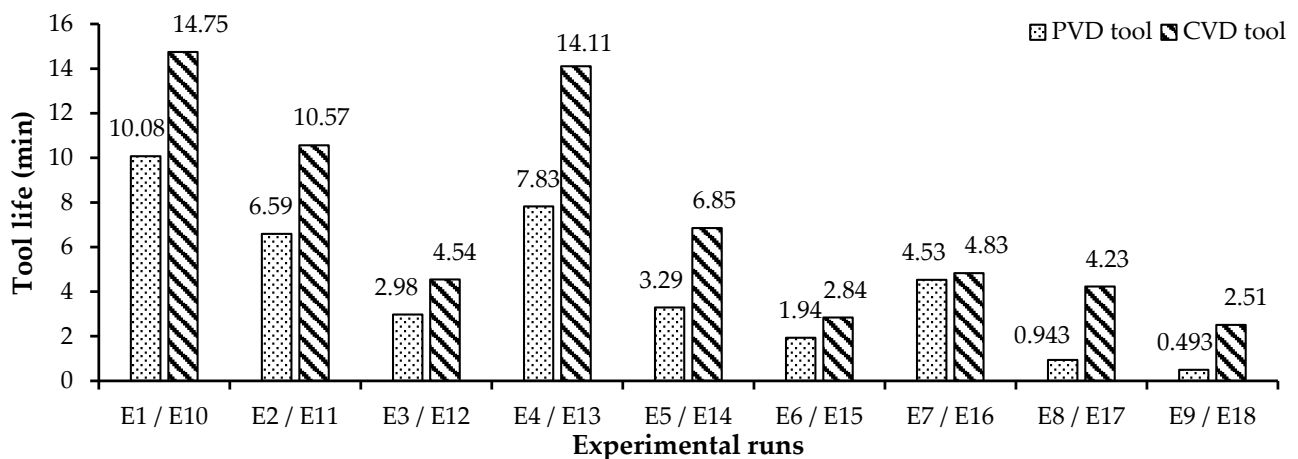


Figure 3. Tool life results for CVD and PVD tools in different experimental runs.

It is evident from Figure 4 that variation in machining parameters can substantially influence the evaluation of tool wear. Most particularly, as the level of cutting speed and feed rate increases, the tool wear accelerates and rapidly progresses towards the severe wear stage for both types of tools. The corresponding wear graphs in Figure 4a–c were, therefore, more skewed towards the left side as the cutting speed increased from 300 to 400 m/min and feed rate increased from 0.05 to 0.15 mm/rev. The most critical reason for this behavior was the excess heat generation with increasing cutting speed, resulting in plastic deformation and thermal softening of the tool material. Even a small rise in the feed rate in this scenario resulted in a proportional increase in the tool's transverse speed across the rotating workpiece, causing friction between the tool and the workpiece, ultimately leading to degradation of the tool [43]. It was noticed that the progression of wear in the case of CVD tools remained nearly steady in all cutting speed and feed rate combinations. However, it notably accelerated for PVD tools when the feed value was raised to 0.1 mm/rev and 0.15 mm/rev, as evident from Figure 4b,c. In order to determine why CVD tools outperformed PVD tools, microscopic and SEM images of worn tools were analyzed with respect to machining time for low and high parametric settings, as shown in Figure 5. It was discernible that PVD tools in both cutting conditions (experiment 1 and 9)

were highly affected by excessive chipping and abrasion, even during the initial wear stage ($V_b \geq 66.21 \mu\text{m}$), indicating that the thin layer of the TiAlN/AlCrN coating ($3 \mu\text{m}$) could not protect the tool against thermal–mechanical loads. On the contrary, the double thick layer of the $\text{Al}_2\text{O}_3/\text{TiCN}$ coating ($18 \mu\text{m}$) showed better resistance to chipping during the initial and gradual wear stages. It could also be observed from the tool cutting geometry in Figure 5 that it was relatively more stable at high wear width, $V_b \leq 194.14 \mu\text{m}$ @ 8.2 min in experiment 10 and at $V_b \leq 167.33 \mu\text{m}$ @ 1.83 min in experiment 18. According to Sonawane and Sargade [25], thicker coatings have low thermal conductivity, which plays a crucial role in protecting the carbide substrate from exposure to temperature variation. However, soon after the deterioration of the coating, the carbide substrate of both tools could not withstand the thermal–mechanical variations imposed by harsh machining conditions. Thus, they experienced faster progression towards the failure region. It is worth noting that PVD tools exhibited less flank wear width than CVD tools in experiment 1 ($V_b = 339.70 \mu\text{m} < V_b = 366.18 \mu\text{m}$) and experiment 9 ($V_b = 415.2 \mu\text{m} < V_b = 841.12 \mu\text{m}$). This behavior could be attributed to the following reasons:

- Comparatively lower depth of cut of 0.1 mm for the PVD tool, which exerted less mechanical load on the tool edge, eventually causing less damage.
- The higher hardness possessed by the PVD tool (93.2 HRA) compared to the CVD tool (90.5 HRA), which provided stability against thermal–mechanical loads.
- The high thermal expansion coefficient of the inner coating in case of the CVD tool ($\text{TiCN} \sim 7.8 \times 10^{-6} \text{ K}^{-1}$ [44] > $\text{AlCrN} \sim 6 \times 10^{-6} \text{ K}^{-1}$ [45]) compared to the carbide substrate ($5.7\text{--}6.9 \times 10^{-6} \text{ K}^{-1}$ [46]), causing the coating to expand more than the carbide substrate. Consequently, this exerted compressive stresses and damaged the tool.
- The high thermal conductivity of the TiCN coating (30 W/mk [47]) compared to AlCrN (4.63 W/mk [48]), causing excess heat to transfer to the carbide substrate, thereby weakening the base material of the tool and resulting in extensive flank wear.

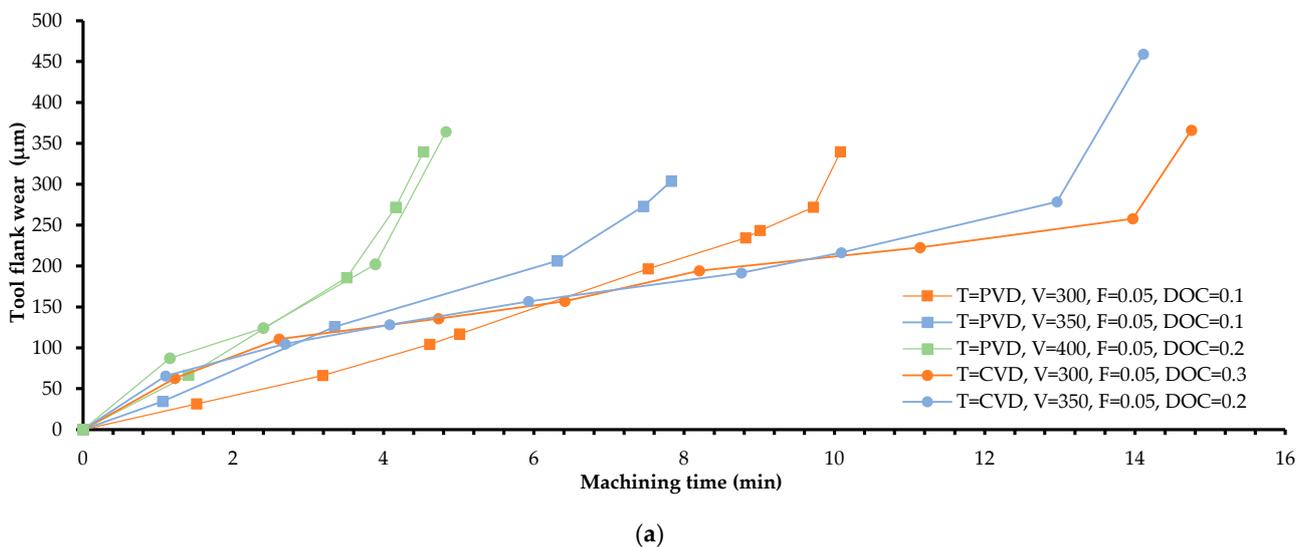


Figure 4. Cont.

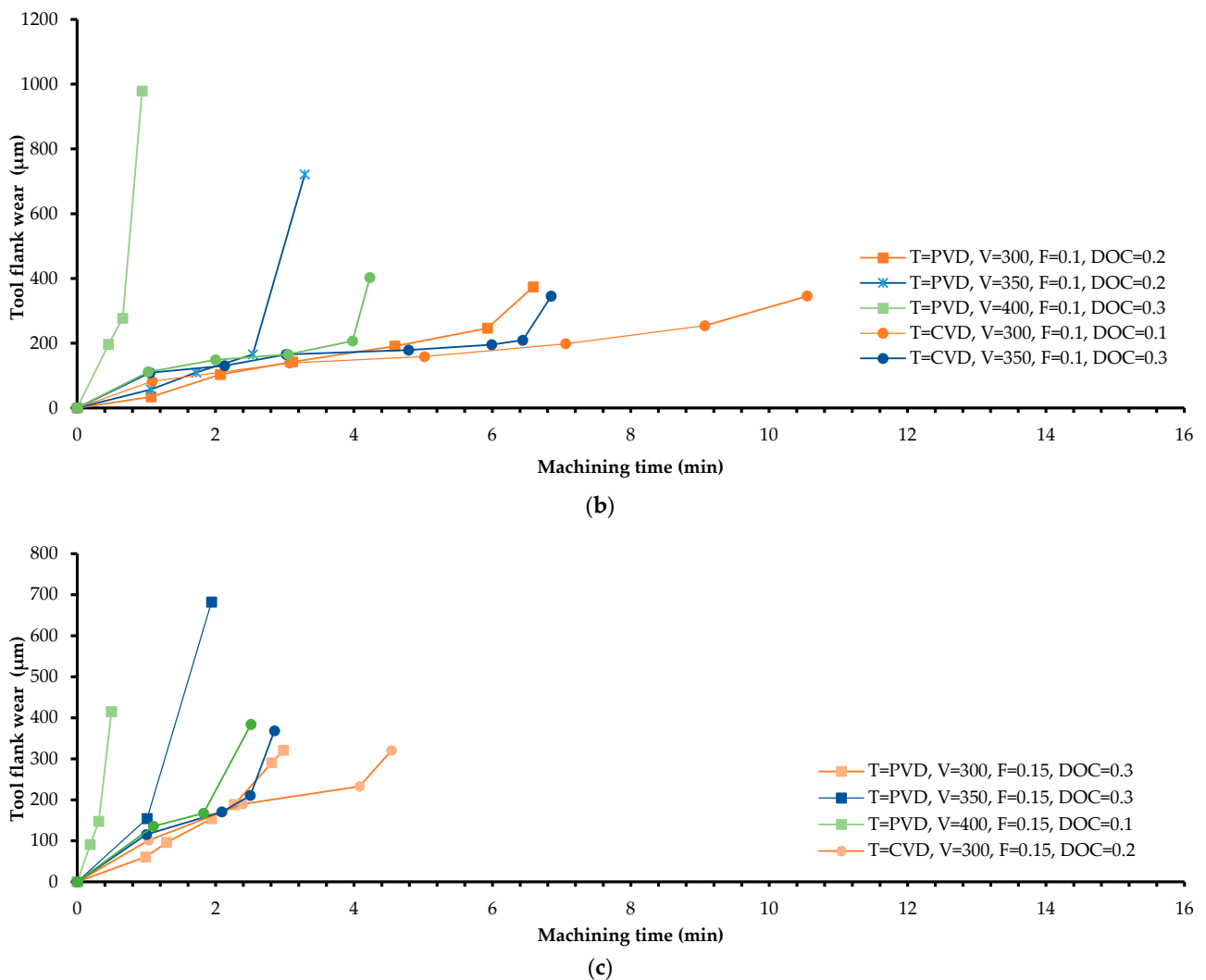


Figure 4. Wear progression for PVD and CVD tools at feed rates of (a) 0.05 mm/rev, (b) 0.1 mm/rev, and (c) 0.15 mm/rev.

3.2.2. Tool Wear Mechanisms

To comprehend the wear mechanisms for both types of tools, SEM analysis was performed on the worn tool from experiments 1 and 10. Three regions of the worn tools were also examined in detail for SEM and EDX analysis: (a) crater face, (b) cutting edge, and (c) flank face. Figure 6a represented the high crater formation of the PVD tool, indicating a severe tribological condition between the flowing chips and the tool rake face. Reis et al. [49] stated that the combined effect of diffusion and adhesion caused the evolution of crater wear. Traces of elemental composition in spectra 1 and 2 showed the strong peaks of Fe and an appreciable amount of oxygen. This confirmed the adherence of the workpiece material, as well as elemental diffusion and oxidation, which were likely caused by the formation of iron oxide and a high-stress field at elevated temperature. Since the machining was performed in a high-speed regime, the generation of intense heat was inevitable. The rough surface on the crater surface also indicated diffusion. Moreover, chipping and abrasion were also noticed near the cutting edge. The presence of a few traces of Ti and Al elements in all spectra suggested that the tool coating had deteriorated. However, a noticeable percentage of W in spectra 1 and 2 represented exposure to the carbide substrate. It was expected that the periodic entry of the tool during the cutting cycle may have smashed the adhered material onto the tool, thereby leading to carbide breakage in the form of chipping. Das et al. [50] stated that stress concentration and uneven force distribution near the cutting

edge increase the possibility of chipping followed by tool fracture. Parallel friction marks in the direction of material flow indicated abrasion, which was identifiable on the tool flank face near the main cutting edge. The hard carbide micro-inclusion in the workpiece material rubbed against the tool, which caused abrasive wear. Furthermore, a significant percentage of workpiece material in spectra 1 and 2 indicated serious adhesion and was a possible cause of accelerated tool flank wear in the case of the PVD tool.

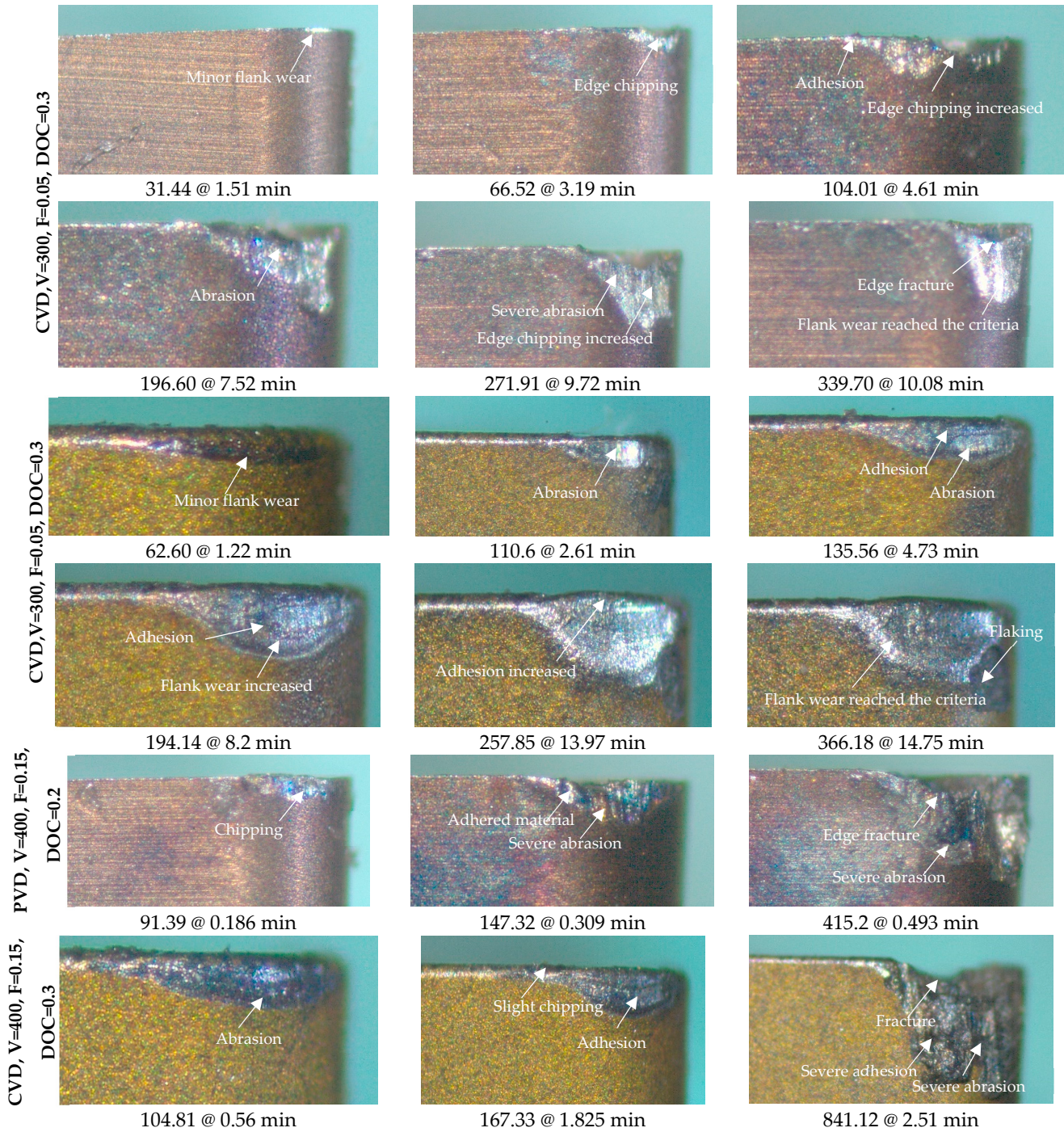
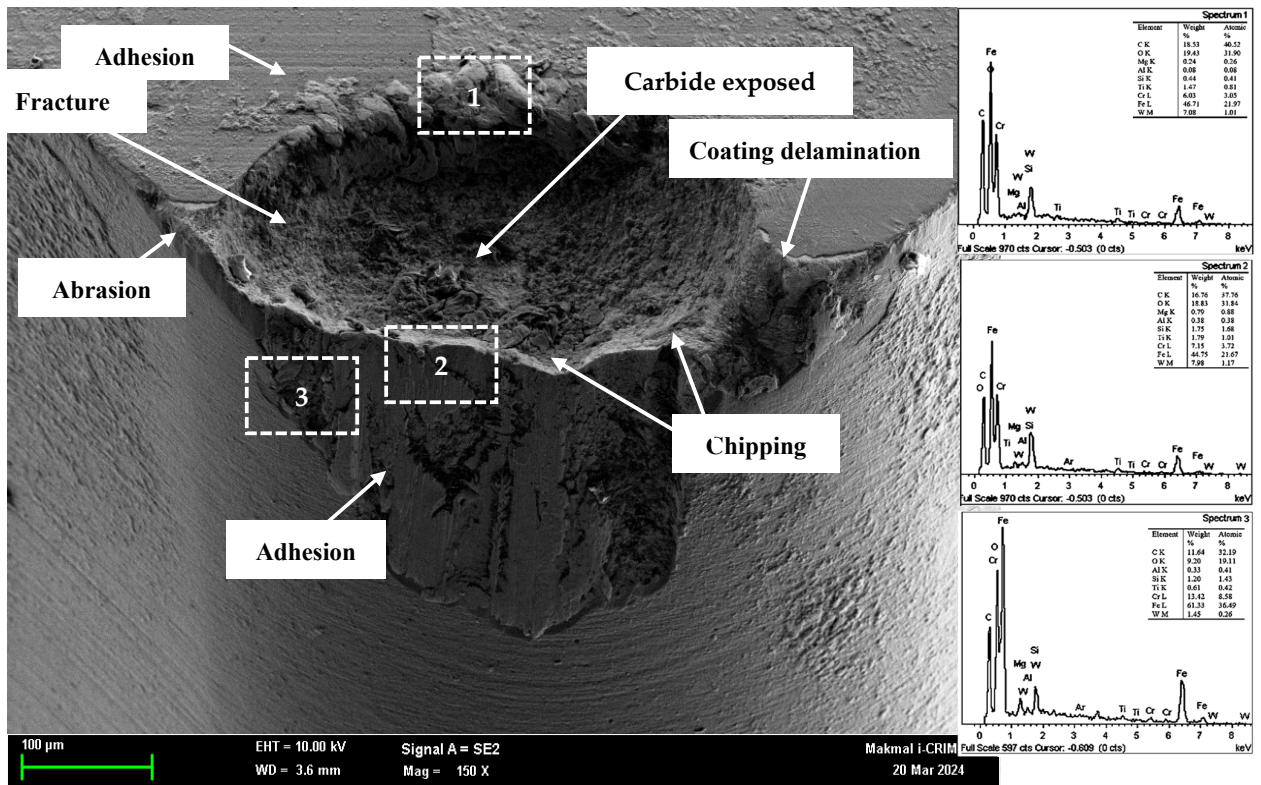
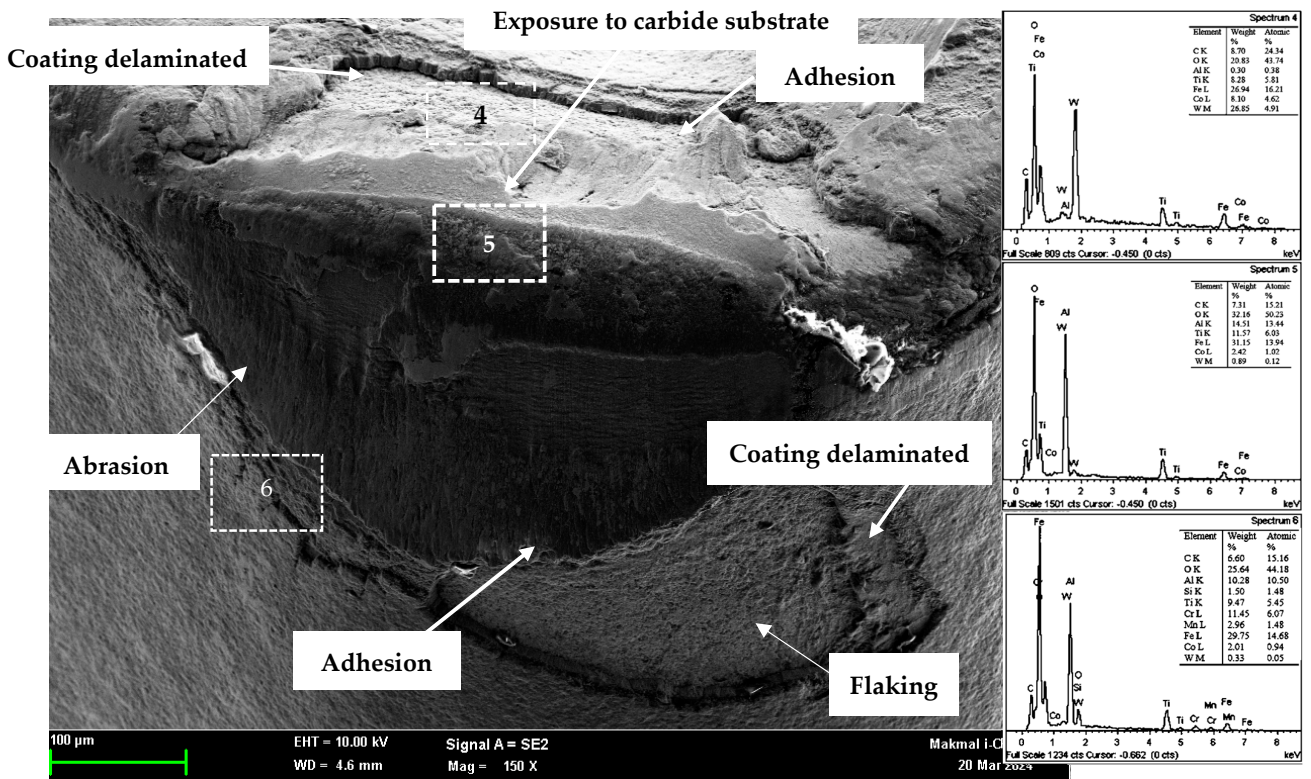


Figure 5. Wear images of both tools with the machining time at low and high parametric settings.



(a)



(b)

Figure 6. SEM and EDX analysis of the worn tools at $V = 300$ m/min and $F = 0.05$ mm/rev. (a) PVD tool; (b) CVD tool.

In comparison, the CVD tool exhibited a shallower crater depth, as shown in Figure 6b. This was due to the effective multilayer coating, which substantially minimized the wear and friction in comparison to the PVD tools. However, the EDX analysis of spectrum 4 showed high percentages of W, Co, and O, with a few traces of Al, suggesting the deterioration of the Al_2O_3 coating and the occurrence of oxidation wear. Interestingly, the presence of the inner TiCN coating on the rake face benefitted the carbide substrate against the varied thermo-mechanical loads and caused less damage, as compared to the PVD tool. Therefore, the profile of the main edge was relatively more stable. Previous studies have also reported that the TiCN coating exhibits excellent shock resistance capabilities [51]. The EDX analysis on the cutting edge (spectrum 5) revealed the existence of the $\text{Al}_2\text{O}_3/\text{TiCN}$ coating, which effectively prevented material adhesion and chipping, thereby maintaining a stable cutting-edge geometry. Bjerke et al. [52] stated that the outer layer of the Al_2O_3 coating can form a protective layer of aluminum oxide during the machining process, thus providing thermal stability and abrasion resistance to the cutting edge. The wear morphology at the flank face represents abrasion and adhesion to the tool due to constant rubbing of hard micro-inclusions from the workpiece and carbide substrate. Meanwhile, the adherence on the flank face (as evident from spectrum 6) was an extrusion of flowing chips between the tool and workpiece. Due to the strong chemical affinity of the work material with the tool substrate, further adherence led to the weakening of the binder in the carbide matrix, while the adhered material, being unstable in nature, was continuously dislodged from the tool surface, promoting a traction effect, causing interlayer coating delamination [53]. Considering this fact, it was expected that the high depth of cut in this scenario exerted an increased cutting force, which was sufficiently high to cause tool flaking and ultimately led to the complete tool life criteria.

Based on SEM and EDX analysis, it is summarized that adhesion, oxidation, and abrasion constituted the primary wear mechanisms for both $\text{Al}_2\text{O}_3/\text{TiCN}$ -CVD- and $\text{TiAlN}/\text{AlCrN}$ -PVD-coated tools. However, excessive chipping on the main cutting edge and severe diffusion on the crater face were the contributing factors that accelerated wear mechanisms in the case of the PVD-coated tools.

3.3. Analysis of Surface Roughness for PVD- and CVD-Coated Carbide Tool

A pictorial representation of average surface roughness (R_a) for PVD and CVD tools is shown in Figure 7. It can be seen that the best surface roughness of $0.276 \mu\text{m}$ was obtained with the PVD tool in experiment 4 at $V = 350 \text{ m/min}$, $F = 0.05 \text{ mm/rev}$, and $\text{DOC} = 0.1 \text{ mm}$. However, the minimum R_a of $0.307 \mu\text{m}$ in the case of the CVD tool was obtained at a cutting speed of 400 m/min , feed rate of 0.05 mm/rev , and depth of cut of 0.3 mm . Overall, CVD tools outperformed in delivering the best surface quality, showing 66.6% better results than PVD tools. These results were consistent with the tool wear/life findings discussed in Section 3.2, where the thick layer of the $\text{Al}_2\text{O}_3/\text{TiCN}$ coating effectively decreased the coefficient of friction and resulted in lower surface roughness. On the contrary, the PVD tool was only 33.33% effective in delivering a better surface finish, as per the results of experiments 1, 4, and 7. This meant that the PVD tool with high hardness and a thin coating ($\text{TiAlN}/\text{AlCrN}$) was merely effective at low machining parameters because all these experiments were conducted at a low machining speed $V = 300 \text{ m/min}$, low feed rate 0.05 mm/rev , and low depth of cut, $\text{DOC} = 0.2\text{--}0.3 \text{ mm}$.

From Figure 7, it is also inferred that with an increase in the machining speed, there was a decrease in surface roughness. This is because increasing the speed minimizes the tool–chip contact area, thereby lowering the friction, and this produces better surface quality. Thermal softening of the work material by increasing the cutting speed is one of the governing factors, contributing to a decreasing cutting force as well as decreasing peaks and valleys present in the work surface, thereby allowing for a better surface finish [27]. It was also revealed that the surface roughness for both tools substantially increased with an increment in the feed rate. Most importantly, the value of R_a was augmented at a higher feed $F = 0.15 \text{ mm/rev}$ for both tools due to higher undeformed chip thickness,

which exerted a load on the cutting edge, leading to tool wear and increased surface roughness. The highest R_a of 1.97 μm and 1.211 μm were observed at low machining speeds $V = 300$ m/min and the highest feed rate $F = 0.15$ mm/rev for the PVD and CVD tools, respectively, in experiments 3 and 12. Though the effect of the cutting depth was not statistically significant, as discussed in Section 3.1.2, its higher value with high feed rates (0.1 mm/rev and 0.15 mm/rev) considerably increased the surface roughness. A combination of higher feed rate and depth of cut resulted in an increase in the chip cross-sectional area, which is associated with a higher force requirement to shear the material, resulting in chatter and a subsequent deterioration in surface quality [54]. Hence, it is suggested that a high machining speed with a low feed rate and depth of cut is favorable for lower surface roughness.

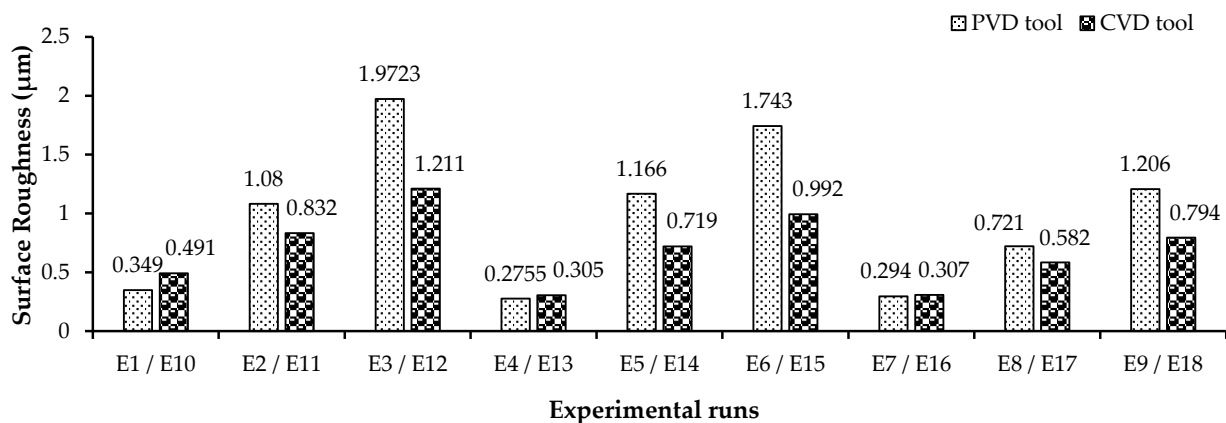


Figure 7. Surface roughness results for PVD and CVD tools in different experimental runs.

4. Conclusions

In this study, the performance of PVD and CVD multilayer-coated tools was analyzed with respect to the tool life, tool wear, and surface roughness undergoing high-speed turning under a dry environment. The following conclusions can be drawn based on this analysis:

1. Based on the ANOVA results, it was found that the feed rate, cutting speed, and tool type significantly influence both the tool life and surface roughness. The feed rate exhibited the highest percentage contributions of 46.22% and 68.96% for tool life and surface roughness, respectively, thereby establishing it as the most influential parameter in this study. However, the cutting depth, with a high p -value (>0.05), was found to be insignificant for both response variables.
2. The highest tool lives of 14.75 min and 10.08 min were obtained at a low cutting speed (300 m/min) and low feed rate (0.05 mm/rev) for CVD- and PVD-coated tools, respectively. The wear progression graph for both tools skewed towards the left as the machining speed and feed rate increased. Additionally, optical microscopic images captured at different time intervals of the worn tool indicated that the CVD-coated tool with the $\text{Al}_2\text{O}_3/\text{TiCN}$ coating protected the tool from thermal-mechanical loads, thus maintaining the cutting-edge geometry, despite high flank wear width at the end of the tool life. Conversely, the PVD tool with the $\text{TiAlN}/\text{AlCrN}$ coating exhibited excessive chipping in the early phases of cutting, resulting in a comparatively shorter tool life.
3. SEM and EDX analysis revealed that adhesion, oxidation, and abrasion constituted the primary wear mechanisms for both types of tools. Furthermore, excessive chipping on the main cutting edge and severe diffusion on the crater face were also identified as contributing factors to the wear mechanisms in the case of PVD-coated tools.
4. The best surface roughness of 0.276 μm and 0.307 μm was achieved at a high cutting speed and low feed rate for both PVD and CVD tools, respectively. Remarkably,

the CVD-coated tool exhibited the most favorable outcomes in terms of low surface roughness due to the reduced thermal conductivity of the Al₂O₃/TiCN coating, which notably reduced the coefficient of friction.

5. From the perspective of future research, a more comprehensive understanding of tool wear mechanisms can be achieved by analyzing the cutting force, chip formation, and cutting temperature. This deeper knowledge is crucial for optimizing the tool life and surface integrity in high-speed machining applications. Additionally, emerging trends in the field of tool coating, for instance, advanced multilayer composite coatings and nano-structural hard coatings, can offer outstanding tribological features and wear resistance to cutting tools. Thus, research in this domain can improve the cutting performances of the PVD- and CVD-coated tools during the machining of high-strength steel. Lastly, the cost quantification and sustainability assessment of coated carbide tools in machining high-strength steel could demonstrate significant economic and environmental benefits, motivating manufacturers to implement these tools in wide-scale industrial applications.

Author Contributions: S.Y.: Methodology, investigation, data curation, writing—original draft. J.A.G.: Methodology, investigation, data curation, writing—review and editing, supervision. N.J.: Writing—review and editing, funding acquisition. A.Z.J.: Writing—review and editing, supervision. All authors have read and agreed to the published version of the manuscript.

Funding: The authors extend their appreciation to Prince Sattam bin Abdulaziz University for funding this research, with project number (PSAU/2024/01/29747).

Institutional Review Board Statement: Not applicable.

Informed Consent Statement: Not applicable.

Data Availability Statement: Data are contained within the article.

Conflicts of Interest: The authors declare no conflicts of interest.

References

1. Musavi, S.H.; Davoodi, B. Risk Assessment for Hazardous Lubricants in Machining Industry. *Environ. Sci. Pollut. Res.* **2021**, *28*, 625–634. [CrossRef]
2. Naveed, M.; Arslan, A.; Javed, H.M.A.; Manzoor, T.; Quazi, M.M.; Imran, T.; Zulfattah, Z.M.; Khurram, M.; Fattah, I.M.R. State-of-the-Art and Future Perspectives of Environmentally Friendly Machining Using Biodegradable Cutting Fluids. *Energies* **2021**, *14*, 4816. [CrossRef]
3. Bagaber, S.A.; Yusoff, A.R. Multi-Objective Optimization of Cutting Parameters to Minimize Power Consumption in Dry Turning of Stainless Steel 316. *J. Clean. Prod.* **2017**, *157*, 30–46. [CrossRef]
4. Yaqoob, S.; Ghani, J.A.; Juri, A.Z.; Muhamad, S.S.; Haron, C.H.C.; Jouini, N. A Review of Sustainable Hybrid Lubrication (Cryo-MQL) Techniques in Machining Processes. *Int. J. Adv. Manuf. Technol.* **2024**, *131*, 151–169. [CrossRef]
5. Dedalus Consulting. Global Market Research End User Analysis Database. 2022. Available online: <https://www.dedalusconsulting.com/index.php> (accessed on 20 January 2024).
6. Boing, D.; De Oliveira, A.J.; Schroeter, R.B. Evaluation of Wear Mechanisms of PVD and CVD Coatings Deposited on Cemented Carbide Substrates Applied to Hard Turning. *Int. J. Adv. Manuf. Technol.* **2020**, *106*, 5441–5451. [CrossRef]
7. Dabees, S.; Mirzaei, S.; Kaspar, P.; Holcman, V.; Sobola, D. Characterization and Evaluation of Engineered Coating Techniques for Different Cutting Tools—Review. *Materials* **2022**, *15*, 5633. [CrossRef]
8. Sousa, V.F.C.; Silva, F.J.G. Recent Advances in Turning Processes Using Coated Tools—A Comprehensive Review. *Metals* **2020**, *10*, 170. [CrossRef]
9. Panjan, P.; Drnovšek, A.; Terek, P.; Miletić, A.; Čekada, M.; Panjan, M. Comparative Study of Tribological Behavior of TiN Hard Coatings Deposited by Various PVD Deposition Techniques. *Coatings* **2022**, *12*, 294. [CrossRef]
10. Von Fieandt, L.; Johansson, K.; Larsson, T.; Boman, M.; Lindahl, E. On the Growth, Orientation and Hardness of Chemical Vapor Deposited Ti (C, N). *Thin Solid Film.* **2018**, *645*, 19–26. [CrossRef]
11. Chinchani, S.; Choudhury, S.K. Wear Behaviors of Single-Layer and Multi-Layer Coated Carbide Inserts in High Speed Machining of Hardened AISI 4340 Steel. *J. Mech. Sci. Technol.* **2013**, *27*, 1451–1459. [CrossRef]
12. Feng, R.; Pan, J.; Zhang, J.; Shao, Y.; Chen, B.; Fang, Z.; Roy, K.; Lim, J.B.P. Effects of Corrosion Morphology on the Fatigue Life of Corroded Q235B and 42CrMo Steels: Numerical Modelling and Proposed Design Rules. *Structures* **2023**, *57*, 105136. [CrossRef]
13. Feng, R.; Yang, F.; Shao, Y.; Roy, K.; Lim, J.; Chen, B. Experimental Study on High-Cycle Fatigue Behaviour of Butt Welds Made of Corroded AISI 304 Stainless Steel and Q460 High-Strength Steel. *Structures* **2024**, *62*, 106141. [CrossRef]

14. Muhamad, S.S.; Ghani, J.A.; Che Haron, C.H.; Yazid, H. Wear Mechanism of Multilayer Coated Carbide Cutting Tool in the Milling Process of AISI 4340 under Cryogenic Environment. *Materials* **2022**, *15*, 524. [CrossRef] [PubMed]
15. Yap, P.H.; Ghani, J.A.; Wan Mahmood, W.M.F. Optimisation on the Performance of Bubble-Bursting Atomisation for Minimum Quantity Lubrication with Vegetable Oil Using Computational Fluid Dynamics Simulation. *Materials* **2022**, *15*, 4355. [CrossRef] [PubMed]
16. Abu Bakar, H.N.; Ghani, J.A.; Haron, C.H.C.; Ghazali, M.J.; Kasim, M.S.; Al-Zubaidi, S.; Jouini, N. Wear Mechanisms of Solid Carbide Cutting Tools in Dry and Cryogenic Machining of AISI H13 Steel with Varying Cutting-Edge Radius. *Wear* **2023**, *523*, 204758. [CrossRef]
17. Xu, Q.; Zhao, J.; Ai, X. Cutting Performance of Tools Made of Different Materials in the Machining of 42CrMo4 High-Strength Steel: A Comparative Study. *Int. J. Adv. Manuf. Technol.* **2017**, *93*, 2061–2069. [CrossRef]
18. Ahmad, A.A.; Ghani, J.A.; Che Haron, C.H. Effect of Cutting Parameters on Tool Life during End Milling of AISI 4340 under MQL Condition. *Ind. Lubr. Tribol.* **2022**, *74*, 392–401. [CrossRef]
19. Yang, W.; Xiong, J.; Guo, Z.; Du, H.; Yang, T.; Tang, J.; Wen, B. Structure and Properties of PVD TiAlN and TiAlN/CrAlN Coated Ti (C, N)-Based Cermets. *Ceram. Int.* **2017**, *43*, 1911–1915. [CrossRef]
20. Kenzhegulov, A.; Mamaeva, A.; Panichkin, A.; Alibekov, Z.; Kshibekova, B.; Bakhytuly, N.; Wieleba, W. Comparative Study of Tribological and Corrosion Characteristics of TiCN, TiCrCN, and TiZrCN Coatings. *Coatings* **2022**, *12*, 564. [CrossRef]
21. Li, Y.; Zheng, G.; Cheng, X.; Yang, X.; Xu, R.; Zhang, H. Cutting Performance Evaluation of the Coated Tools in High-Speed Milling of AISI 4340 Steel. *Materials* **2019**, *12*, 3266. [CrossRef]
22. Das, A.; Patel, S.K.; Hotta, T.K.; Biswal, B.B. Statistical Analysis of Different Machining Characteristics of EN-24 Alloy Steel during Dry Hard Turning with Multilayer Coated Cermet Inserts. *Measurement* **2019**, *134*, 123–141. [CrossRef]
23. Zheng, G.; Cheng, X.; Li, L.; Xu, R.; Tian, Y. Experimental Investigation of Cutting Force, Surface Roughness and Tool Wear in High-Speed Dry Milling of AISI 4340 Steel. *J. Mech. Sci. Technol.* **2019**, *33*, 341–349. [CrossRef]
24. Davoodi, B.; Eskandari, B. Tool Wear Mechanisms and Multi-Response Optimization of Tool Life and Volume of Material Removed in Turning of N-155 Iron–Nickel-Base Superalloy Using RSM. *Measurement* **2015**, *68*, 286–294. [CrossRef]
25. Sonawane, G.D.; Sargade, V.G. Machinability Study of Duplex Stainless Steel 2205 During Dry Turning. *Int. J. Precis. Eng. Manuf.* **2020**, *21*, 969–981. [CrossRef]
26. Bag, R.; Panda, A.; Sahoo, A.K.; Kumar, R. Sustainable High-Speed Hard Machining of AISI 4340 Steel under Dry Environment. *Arab. J. Sci. Eng.* **2022**, *48*, 3073–3096. [CrossRef]
27. Alok, A.; Kumar, A.; Das, M. Hard Turning with a New HSN2-Coated Carbide Insert and Optimization of Process Parameter. *Trans. Indian. Inst. Met.* **2021**, *74*, 1577–1591. [CrossRef]
28. Kumar, S.; Singh, D.; Kalsi, N.S. Performance Evaluation of TiN-Coated CBN Tools During Turning of Variable Hardened AISI 4340 Steel. In *Advanced Engineering Optimization through Intelligent Techniques*; Venkata Rao, R., Taler, J., Eds.; Advances in Intelligent Systems and Computing; Springer: Singapore, 2020; Volume 949, pp. 847–857. ISBN 9789811381959.
29. Singh, R.; Dureja, J.S.; Dogra, M. Performance Evaluation of Textured Carbide Tools under Environment-Friendly Minimum Quantity Lubrication Turning Strategies. *J. Braz. Soc. Mech. Sci. Eng.* **2019**, *41*, 87. [CrossRef]
30. Jafarian Zenjanab, M.; Pedrammehr, S.; Chalak Qazani, M.R.; Shabgard, M.R. Influence of Cutting Fluid-Based CuO-Nanofluid with Boric Acid-Nanoparticles Additives on Machining Performances of AISI 4340 Tool Steel in High-Speed Turning Operation. *Iran. J. Sci. Technol. Trans. Mech. Eng.* **2022**, *46*, 335–345. [CrossRef]
31. Shalaby, M.; Veldhuis, S. New Observations on High-Speed Machining of Hardened AISI 4340 Steel Using Alumina-Based Ceramic Tools. *J. Manuf. Mater. Process.* **2018**, *2*, 27. [CrossRef]
32. Suyama, D.I.; Diniz, A.E. Influence of Tool Vibrations on Tool Wear Mechanisms in Internal Turning of Hardened Steel. *J. Braz. Soc. Mech. Sci. Eng.* **2020**, *42*, 370. [CrossRef]
33. Da Silva, L.R.; Couto, D.A.; Dos Santo, F.V.; Duarte, F.J.; Mazzaro, R.S.; Veloso, G.V. Evaluation of Machined Surface of the Hardened AISI 4340 Steel through Roughness and Residual Stress Parameters in Turning and Grinding. *Int. J. Adv. Manuf. Technol.* **2020**, *107*, 791–803. [CrossRef]
34. Tang, S.; Liu, P.; Su, Z.; Lei, Y.; Liu, Q.; Liu, D. Preparation and Cutting Performance of Nano-Scaled Al₂O₃-Coated Micro-Textured Cutting Tool Prepared by Atomic Layer Deposition. *High Temp. Mater. Process.* **2021**, *40*, 77–86. [CrossRef]
35. Gupta, K.M.; Ramdev, K.; Dharmateja, S.; Sivarajan, S. Cutting Characteristics of PVD Coated Cutting Tools. *Mater. Today Proc.* **2018**, *5*, 11260–11267. [CrossRef]
36. Alaksanasuwan, S.; Buranawong, A.; Witit-Anun, N. Preparation and Characterization of Nanostructured TiCrN Thin Films Deposited from Ti-Cr Mosaic Target by Reactive DC Magnetron Sputtering. *J. Phys. Conf. Ser.* **2021**, *1719*, 012072. [CrossRef]
37. ISO 3685:1993; Tool-Life Testing with Single-Point Turning Tools. International Organization for Standardization (ISO): Geneva, Switzerland, 1993.
38. Sumitomo, E. Sumitomo Cutting Tools General Catalog 2023–2024. 2023. Available online: <https://www.sumitool.com/en/downloads/cutting-tools/general-catalog> (accessed on 15 August 2023).
39. López-Luiz, N.; Alemán, O.J.; Hernández, F.A.; Dávila, M.M.; Baltazar-Hernández, V.H. Experimentation on Tool Wear and Surface Roughness in AISI D2 Steel Turning with WC Insert. *Mod. Mech. Eng.* **2018**, *8*, 204–220. [CrossRef]
40. Fedai, Y. Exploring the Impact of the Turning of AISI 4340 Steel on Tool Wear, Surface Roughness, Sound Intensity, and Power Consumption under Dry, MQL, and Nano-MQL Conditions. *Lubricants* **2023**, *11*, 442. [CrossRef]

41. Mia, M.; Dey, P.R.; Hossain, M.S.; Arafat, M.T.; Asaduzzaman, M.; Ullah, M.S.; Zobaer, S.T. Taguchi S/N Based Optimization of Machining Parameters for Surface Roughness, Tool Wear and Material Removal Rate in Hard Turning under MQL Cutting Condition. *Measurement* **2018**, *122*, 380–391. [[CrossRef](#)]
42. Butt, M.M.; Najar, K.A.; Dar, T.H. Experimental Evaluation of Multilayered CVD-and PVD-Coated Carbide Turning Inserts in Severe Machining of AISI-4340 Steel Alloy. *J. Tribol.* **2021**, *29*, 117–143.
43. Li, Y.; Zheng, G.; Zhang, X.; Cheng, X.; Yang, X.; Xu, R. Cutting Force, Tool Wear and Surface Roughness in High-Speed Milling of High-Strength Steel with Coated Tools. *J. Mech. Sci. Technol.* **2019**, *33*, 5393–5398. [[CrossRef](#)]
44. Xian, G.; Xiong, J.; Zhao, H.; Xian, L.; Fan, H.; Li, Z.; Du, H. Study on the Growth and Wear Behavior of the TiAlN-Based Composite Coating Deposited on TiCN-Based Cermets with Different Binder Phase. *Wear* **2020**, *460–461*, 203460. [[CrossRef](#)]
45. Bartosik, M.; Daniel, R.; Mitterer, C.; Keckes, J. Thermally-Induced Formation of Hexagonal AlN in AlCrN Hard Coatings on Sapphire: Orientation Relationships and Residual Stresses. *Surf. Coat. Technol.* **2010**, *205*, 1320–1323. [[CrossRef](#)]
46. Stylianou, R.; Velic, D.; Daves, W.; Ecker, W.; Tkadletz, M.; Schalk, N.; Czettel, C.; Mitterer, C. Thermal Crack Formation in TiCN/ α -Al₂O₃ Bilayer Coatings Grown by Thermal CVD on WC-Co Substrates with Varied Co Content. *Surf. Coat. Technol.* **2020**, *392*, 125687. [[CrossRef](#)]
47. Kone, F.; Czarnota, C.; Haddag, B.; Nouari, M. Finite Element Modelling of the Thermo-Mechanical Behavior of Coatings under Extreme Contact Loading in Dry Machining. *Surf. Coat. Technol.* **2011**, *205*, 3559–3566. [[CrossRef](#)]
48. Samani, M.K.; Chen, G.C.K.; Ding, X.Z.; Zeng, X.T. Thermal Conductivity of CrAlN and TiAlN Coatings Deposited by Lateral Rotating Cathode Arc. *Key Eng. Mater.* **2010**, *447–448*, 705–709. [[CrossRef](#)]
49. Reis, B.C.M.; Dos Santos, A.J.; Dos Santos, N.F.P.; Câmara, M.A.; De Faria, P.E.; Abrão, A.M. Cutting Performance and Wear Behavior of Coated Cermet and Coated Carbide Tools When Turning AISI 4340 Steel. *Int. J. Adv. Manuf. Technol.* **2019**, *105*, 1655–1663. [[CrossRef](#)]
50. Das, A.; Gupta, M.K.; Das, S.R.; Panda, A.; Patel, S.K.; Padhan, S. Hard Turning of AISI D6 Steel with Recently Developed HSN2-TiAlxN and Conventional TiCN Coated Carbide Tools: Comparative Machinability Investigation and Sustainability Assessment. *J. Braz. Soc. Mech. Sci. Eng.* **2022**, *44*, 138. [[CrossRef](#)]
51. Patil, P.; Karande, P. Performance Analysis of Twin-Layer AlTiN and TiCN Coated Inserts during High Speed Turning of SS304 with Synthetic Coolant at 0 °C. *Tribol.—Mater. Surf. Interfaces* **2024**, *18*, 53–62. [[CrossRef](#)]
52. Bjerke, A.; Lenrick, F.; Norgren, S.; Larsson, H.; Markström, A.; M'Saoubi, R.; Petrusha, I.; Bushlya, V. Understanding Wear and Interaction between CVD α -Al₂O₃ Coated Tools, Steel, and Non-Metallic Inclusions in Machining. *Surf. Coat. Technol.* **2022**, *450*, 128997. [[CrossRef](#)]
53. Hassan, S.; Khan, S.A.; Naveed, R.; Saleem, M.Q.; Mufti, N.A.; Farooq, M.U. Investigation on Tool Wear Mechanisms and Machining Tribology of Hardened DC53 Steel through Modified CBN Tooling Geometry in Hard Turning. *Int. J. Adv. Manuf. Technol.* **2023**, *127*, 547–564. [[CrossRef](#)]
54. Saleem, M.Q.; Mumtaz, S. Face Milling of Inconel 625 via Wiper Inserts: Evaluation of Tool Life and Workpiece Surface Integrity. *J. Manuf. Process.* **2020**, *56*, 322–336. [[CrossRef](#)]

Disclaimer/Publisher's Note: The statements, opinions and data contained in all publications are solely those of the individual author(s) and contributor(s) and not of MDPI and/or the editor(s). MDPI and/or the editor(s) disclaim responsibility for any injury to people or property resulting from any ideas, methods, instructions or products referred to in the content.